Direct calculation of inverse-bremsstrahlung absorption in strongly coupled, nonlinearly driven laser plasmas

Susanne Pfalzner
Astrophysikalisches Institut und Sternwarte, Schillergäßchen 3, D-07745 Jena, Germany

Paul Gibbon
Abteilung Röntgenoptik, Insititut für Optik und Quantenelektronik, Max-Wien-Platz 1, D-07743 Jena, Germany

(Received 26 August 1997; revised manuscript received 8 January 1998)

Inverse-bremsstrahlung absorption in strongly coupled plasmas produced by high-intensity lasers is studied numerically. The simultaneous presence of high density and intensity makes it difficult to treat this problem with standard methods. A technique for modeling collisional plasmas is demonstrated which uses a hierarchical tree code—an accelerated molecular dynamics algorithm with an N log N computation time—adapted to model periodic, non-equilibrium two-component plasmas. Good agreement is found with standard theoretical results for classical, weakly coupled plasmas. In a series of further simulations, the dependence of the inverse-bremsstrahlung absorption coefficient on plasma coupling parameter, laser frequency, and the ratio of quiver to thermal velocity v_0/v_{te} is computed. An important outcome of this study is that the Langdon effect—a change of the velocity distribution function due to an imbalance of heating and equilibration rates—is verified in a direct microscopic particle simulation. [S1063-651X(98)10104-6]

PACS number(s): 52.20.Fs, 52.25.Fi, 52.65.−y

I. INTRODUCTION

Understanding collisional processes between particles in dense plasmas is of fundamental importance in predicting the thermodynamic properties of many laboratory and astrophysical plasma systems. This problem has become increasingly important since the development of high-intensity lasers capable of creating simultaneously hot and dense states of matter [1]. The interaction of the particles in dense plasmas differs considerably from classical plasmas and the ideal gas assumption underpinning many theories of thermodynamic properties is no longer justified. An important parameter which characterizes the strength of the interaction between the particles is the ion coupling parameter Γ. It essentially describes the ratio of the potential to the kinetic energy of the particles of the plasma,

$$\Gamma = \frac{Z^2 e^2}{a_i k_B T}, \tag{1}$$

where Z is the ion charge, $a_i = (4\pi n_i/3)^{-1/3}$ is the ion sphere radius, n_i is the ion density, and T is the temperature. If $\Gamma > 1$, the system is said to be strongly coupled. Since classical theory relies on the ability to make expansions in terms of Γ, it is expected that strongly coupled plasmas should exhibit very different behavior in their basic properties such as interparticle correlations, transport coefficients, and atomic physics.

Another important parameter is the degree to which the electron gas is degenerate, given by $\theta_e = k_B T/\epsilon_F$ where $\epsilon_F = \hbar^2(3\pi^2 n_e)^{2/3}/2m_e$ is the Fermi energy and n_e is the electron density. In this paper only nondegenerate plasmas will be considered. This means a two-component plasma consisting of electrons and ions is investigated and both species are treated explicitly. However, the same method with only small modifications could also be applied to one-component plasmas, where only the dynamics of the ions is simulated explicitly and the degenerate electrons are treated as a uniform background charge.

The production of such a plasma by high-intensity laser light poses two additional problems for an accurate theoretical description. The main effect of the high-intensity light on the plasma is the presence of a strong oscillating electric field $E = E_0 \sin\omega t$. The electron excursion length due to this sinusoidal field, $x_0 = eE_L/m_e\omega^2$, can be large in comparison to the screening length within the plasma described by the Debye length, $\lambda_D = (k_B T_e/4\pi e^2 n_e)^{1/2}$. The second problem is that the quiver velocity $v_0 = eE_L/m_e\omega$ due to the field can be comparable to or larger than the thermal velocity $v_{te} = \sqrt{k_B T_e/m_e}$. Both situations mean that standard methods treating either the high density and/or the high intensity as a small perturbation of the system are no longer applicable, and a number of highly nonlinear processes may occur simultaneously. In this paper it will be shown how such systems can be modeled by ''molecular dynamics'' simulation in which both strong coupling and strong electric fields can be included without making any *a priori* assumptions.

Until now, these effects—strong coupling of the plasma, strong external fields, and modification of electron velocity distributions—have been treated separately and/or by perturbational methods. In Sec. II we will first briefly review what has been done to investigate these effects so far, and consider the limitations of these approaches. In Sec. III we describe the numerical method upon which the plasma tree code is based, together with the modifications made in order to perform nonequilibrium calculations.

When studying the interactions between laser light and a plasma experimentally or by simulation methods it is essential to know how the laser energy is deposited in the plasma. An important absorption mechanism occurs via collisional processes, known as inverse bremsstrahlung. It describes the

effect where energy of the electric field induced by the laser is absorbed by the plasma via electron-ion collisions. Inverse bremsstrahlung (IB) plays an important role in the context of x-ray lasers [2], ultrafast x-ray sources [3,4], and laser fusion [5]. In high gain targets where the laser irradiation produces warm long-scale-length plasmas, IB is the dominant absorption process. In Sec. IV we illustrate the versatility of this code by computing inverse-bremsstrahlung absorption across a wide range of Γ, ω, and v_0/v_{te}.

II. THEORY OF COLLISIONAL PLASMA PROCESSES

In the standard theory for inverse-bremsstrahlung absorption assuming the plasma as ideal gas and a weak electric field Dawson and Oberman [6] showed that the absorption coefficient is given by

$$\kappa = 1.89\times 10^{6} T_e^{-1/2} Z^2 N_e N_i \nu^{-3} (1-e^{-h\nu/k_B T_e}) \times (1-\omega_p^2/\omega^2)^{-1/2} \ln\Lambda \ \mathrm{cm}^{-1}, \quad (2)$$

where ν is the photon frequency and $\ln\Lambda$ is the Coulomb logarithm, with $\Lambda = \min\{v_{te}/\omega_p b_{\min}, v_{te}/\omega b_{\min}\}$, and $b_{\min} = Ze^2/k_B T_e$ in the classical limit. However, this formula is limited to the case of $v_0/v_{te} \ll 1$, $x_0 \ll \lambda_D$, low plasma density, and assumes a Maxwellian electron velocity distribution. Naturally there have been various attempts to overcome these limitations. As pointed out before, the different effects of high laser intensity and high density of the plasma have mainly been treated separately.

A. Effect of $v_0/v_{te} \geq 1$

The presence of a high electric field generally results in a reduced collision rate because of the enhanced average electron velocity. The precise magnitude of this reduction factor has been the subject of much attention and debate over the last 20 years [7–11]. More recently, Decker *et al.* [12] extended the high-frequency model of Dawson and Oberman [6] to arbitrary values of the quiver velocity v_0/v_{te} and excursion length x_0/λ_D. Their results agree with those of Silin [13]. The numerical expressions for the extreme cases of the collision frequency are given by

$$\frac{\nu_{ei}}{\omega_p} = 5.15\times 10^{-11} \frac{n^{1/2}}{(k_B T_e)^{3/2}} \ln\Lambda \ \text{for } v_0 < v_{te}, \quad (3)$$

$$\frac{\nu_{ei}}{\omega_p} = 2.5\times 10^{-10} \frac{n^{1/2}}{(k_B T_e)^{3/2}} u^{-3} (\ln u/2 + 1) \ln\Lambda \ \text{for } v_0 > v_{te}, \quad (4)$$

where $u = v_0/v_{te} \simeq 6\times 10^{-7}\sqrt{I\lambda^2/kT_e}$ and the laser intensity I is in units of W/cm^2, the wavelength in μm, n is in cm^{-3}, and kT_e is in eV. They concluded that the error in either of these expressions is not too severe in the region $v_0/v_{te} \sim 1$.

Comparing their results with two-dimensional (2D) particle-in-cell (PIC) simulations, Decker *et al.* find differences between the simulation and the analytical result for $x_0/\lambda_d \gg 1$. They conjecture that the collisions become correlated when the excursion length of the oscillation x_0 becomes large in comparison to the Debye length λ_D.

B. Langdon effect

Langdon [14] predicted that strong electromagnetic radiation in plasmas heated by inverse bremsstrahlung would result in non-Maxwellian velocity distributions. If $\nu_{ee} v_{te} \gg \nu_{ei} v_0$ the velocity distribution remains Maxwellian. However, if the average ion charge is large and/or the laser radiation high, such that $Zv_0^2/v_{te}^2 \sim 1$, it can happen that collisional heating competes with electron-electron collisions, producing a non-Maxwellian velocity distribution. This effect has been verified by numerical (Fokker-Planck) simulations for plasmas with $Z>1$ [15] and for $Z=1$ plasmas in recent experiments using intense microwave radiation [16]. Decker *et al.* recently pointed out that the above condition should be replaced by $Zv_0^2/v_{te}^2 \ll (1+v_0^3/v_{te}^3)$ to take into account the fact that the electron-ion collision frequency is reduced by the quiver motion, whereas the electron-electron collision rate is unaffected, and an initially Maxwellian distribution is then preserved [17]. A modified electron velocity distribution has consequences for many basic plasma properties, such as a reduction of the absorption rate [14], and modification of heat flux [18] as well as instability thresholds and atomic transition rates.

C. High density

The works mentioned so far mainly deal with the effect of strong electric fields on the absorption and electron velocity distribution function but do not treat the effect of strong coupling. It is expected that the IB absorption again shows departures from classical theory in dense plasmas, because the electron-ion collisions can no longer be regarded as isolated events; instead the surrounding charges will greatly influence the energy transfer. Mostovych *et al.* [19] find that the commonly used high-frequency absorption coefficient of Dawson and Oberman derived for $\Gamma \ll 1$ but often extrapolated into the $\Gamma \sim 1$ regime, can underestimate the absorption by as much as a factor of 2 and more. Calculations based on the low-frequency $\ln\Lambda$ and which take the strong coupling into account to some degree—as in the investigations by Cauble and Rozmus [20] and Ichimaru and Tanaka [21]—agree much better with the experimental results.

There are mainly three methods used to deal with the effect of high density on the inverse-bremsstrahlung coefficient and the collision frequency: kinetic theory based on the Kubo expression [22], the Born approximation [23], and density functional theory [24]. Although one can obtain a general formulation of the problem a number of approximations have to be introduced to obtain applicable expressions, for example, the assumption of a Maxwellian velocity distribution and a Debye-Hückel form of the static form factor, which is only valid for weakly coupled plasmas or relatively weak electric field. Rinker [25] developed an extended Ziman formula to give plasma transport coefficients in a tabulated form. This spans a relatively wide range of Γ values and appears to give good agreement with recent conductivity experiments [26].

D. Molecular dynamics methods

It is also possible to investigate strongly coupled plasmas using direct particle-particle simulations. The first such cal-

culations were performed by Brush, Sahlin, and Teller [27] who modeled one-component plasmas (OCP) using Monte Carlo methods. However, the use of Monte Carlo (MC) methods is limited to systems in equilibrium. Fortunately it is possible to investigate systems in equilibrium and nonequilibrium states using a related particle-particle method—molecular dynamics (MD). Hansen *et al.* [28] and Slattery, Doolen, and DeWitt [29] carried out equilibrium calculations using MC and MD methods with improved accuracy.

The main properties investigated to date by MC and MD for dense plasmas have been based on the radial (or ''pair'') distribution function $g(r)$. This describes how likely it is to find a particle at a distance r from another particle, thus giving a measure for the spatial correlation between two particles, and is normalized so that $g(r)$ approaches unity as $r\rightarrow\infty$. The radial distribution is related to the static structure factor $S(k)$ via the Fourier transform. $S(k)$ and $g(r)$ are used to calculate the effects of external forces on the system, where perturbation theory is applicable. However, this is not possible anymore if the external forces are very strong and nonlinear effects become important. In this case the effects have to be measured directly in a system which includes the external force. Here, a two-component plasma is modeled where electrons are only weakly degenerate and are treated the same way as the ions in the simulation.

The problem then reduces to obtaining macroscopic variables with good statistical accuracy and avoiding boundary effects, which means using a large number of particles in a simulation region large enough to encompass physically relevant length scales (for example, the collisional mean free path and the Debye length). With standard MD simulations it is only possible to include a few thousand particles in the calculation for reasonable simulation times. The hierarchical tree method demonstrated here is capable of modeling systems with 10^5–10^6 particles on state-of-the-art computers, thus offering a means of comparing microscopic simulation with theory and experiment.

III. NUMERICAL METHOD

Of the codes developed to study the complex many-body problem of laser beam interaction with targets, the three main types of code in common use, fluid, particle-in-cell, and particle-collision (or Fokker-Planck) codes, are unsuitable for modeling dense plasmas for the following reasons.

Fluid codes treat the plasma as a viscous fluid, where collisions between electrons and ions are included through a damping term. It is assumed that the electron-electron collision rate exceeds the heating rate, so that the distribution function remains Maxwellian. Particle-in-cell codes are traditionally used to model non-Maxwellian phenomena [30,31], but collisions are difficult to include self-consistently.

Particle-collision codes [32–34] solve the Fokker-Planck equation including electron-electron and electron-ion collisions to obtain the electron velocity distribution. The collision term is determined by summation over many small-angle scatterings; it does not take into account very large deflections or encounters between two or more particles. Since none of the above simulation methods can adequately model the situation of interest here, we have to resort to direct methods.

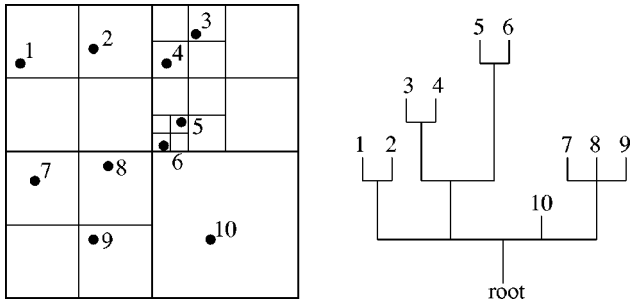

FIG. 1. Construction of two-dimensional tree structure used for storing information on the particle distribution.

The most straightforward computational method would be to follow the paths of all particles of the system induced by the forces due to all particle-particle interactions [35]. However, this becomes prohibitively expensive for large particle numbers, because the computation time is proportional to N^2. Furukawa and Nishihara [36] have investigated absorption using a $\mathrm{P}^3\mathrm{M}$ code, in which the macroscopic field determined by PIC is corrected by calculating forces between nearest neighbors directly [37]. Although numerically efficient, the main drawback with $\mathrm{P}^3\mathrm{M}$ is that it cannot cope well with long-wavelength density perturbations, nor with highly nonlinear clustered systems.

In this paper we use a tree code to simulate a dense plasma. This technique has two advantages over other methods—an accurate handling of collisions, including many-body encounters, large-angle scattering and screening, along with a gridless treatment which in principle permits arbitrary geometry and high-density contrasts.

A. Hierarchical tree method

The tree algorithm we use for plasma simulation is similar to the codes developed for gravitational problems in astrophysics [38,39]. A tutorial account of the numerical realization can be found in [40]. The underlying principle is the following.

The most time consuming part of an N-body code is the force calculation, because taking all particle-particle interactions into account involves $N(N-1)/2$ operations. The basic idea of a hierarchical tree construction is to exploit the $1/r^2$ fall off of the force (in plasmas the effect becomes enhanced by screening). A particle is mainly affected by the force of each particle in its immediate neighborhood and it is sufficient to take particles only groupwise into account at larger distances.

The aim is to avoid calculating the distance between each particle pair, but to develop a relationship between each particle and its neighbors which can function as a measure of closeness. This is achieved by recursively dividing the entire space into subcells until there is only one particle per cell. The resulting data structure is known as the ''tree.'' An example is given in Fig. 1, which shows a distribution of particles with the spatial division and the corresponding tree structure. This structure is used to cluster groups of particles together to pseudoparticles. The influence of remote particles is evaluated from a multipole expansion of the particle clus-

ter rather than its individual members. The force is evaluated for each particle by ''walking'' through the tree, starting at the root and working up towards the leaves. The size of the current cluster is compared with the distance d to the particle of interest by

$$s/d \leqslant \theta,$$

where θ is a tolerance parameter (usually between 0.2 and 1.0). The choice of θ determines whether the force of the charge sum of a cell is evaluated, or whether the cell is split into its daughter cells and the force of each charge sum of the daughter cells calculated. The summation is of course more accurate the more the cell is split, but at a cost of increased computation time. Therefore to maintain a high accuracy and low computational effort at the same time, both the dipole and quadrupole moments of the pseudoparticles are included. For plasmas this is particularly important because quasineutral clusters would be virtually ignored if only monopole terms were taken.

The scheme implemented in our code largely follows that of Makino [41], which enables the particle's interaction lists to be gathered independently of one another. This choice is motivated by the scheme's flexibility, which allows particles to be processed in groups: a feature which permits subcycling of particles with different time steps while maintaining a high level of parallelism.

The simulations are performed using dimensionless units with $m \rightarrow m/m_e$, $q \rightarrow q/e$, $r \rightarrow r/\lambda_D$, $v \rightarrow v/v_{te}$, and $t \rightarrow \omega_p t$, where ω_p is the plasma frequency given by $\omega_p = 4\pi n_e e^2/m_e$. In these units, the force on a particle α can be expressed as

$$m_\alpha \frac{d\boldsymbol{v}_\alpha}{dt} = \frac{1}{3N_D} \sum_{\beta \neq \alpha} \frac{q_\alpha q_\beta \boldsymbol{r}_{\alpha\beta}}{r_{\alpha\beta}^3} + q_\alpha \boldsymbol{E}_0, \tag{5}$$

where $N_D = (4\pi/3) n_e \lambda_D^3$ is the number of electrons in a Debye sphere, and $\boldsymbol{E}_0$ is the externally applied electric field amplitude. For an oscillating laser field $E_L \sin \omega t$, we have $E_0 = \omega v_0 / \omega_p v_{te}$, where v_0 is the quiver velocity as defined earlier. The normalized potential energy ($U \rightarrow U/mv_{te}^2 = U/k_B T_e$) of the system is

$$U_{\text{pot}} = \frac{1}{3N_D} \sum_{\alpha, \beta \neq \alpha} \frac{q_\alpha q_\beta}{r_{\alpha\beta}} \tag{6}$$

and the kinetic energy

$$U_{\text{kin}} = \frac{1}{2} \sum_\alpha m_\alpha v_\alpha^2. \tag{7}$$

The simulation region is set up by placing a number of electrons and ions in a cubic box of length L. The size of this box is defined according to the number of electrons in a Debye sphere. For a given electron density we have

$$n_e = \frac{N_e}{L^3} = \frac{N_D}{(4\pi/3)\lambda_D^3},$$

whence the normalized box length,

$$\widetilde{L} \equiv \frac{L}{\lambda_D} = \frac{4\pi}{3} \frac{N_e}{N_D} = \left(\frac{4\pi N_e}{3} \right)^{1/3} a_e,$$

where a_e is the mean interelectron spacing. Generally it is more convenient to specify Γ and Z rather than a_e, so in practice we define L according to (see the Appendix)

$$L = \left(\frac{4\pi N_e}{3} \right)^{1/3} (3\Gamma)^{1/2} Z^{-5/6} \tag{8}$$

and the ions are placed in the same box with $N_i = N_e/Z$.

Due to the attractive forces between the electrons and ions a ''bare'' Coulombic potential would make the system unstable via stochastic heating. Therefore it is necessary to include a short range truncation which allows this singularity to be dealt with. To retain some physical basis for this, effective pair potentials can be used which can account for quantum diffraction as well as symmetry effects in an approximative way [42]. However, since we are not explicitly interested in degeneracy effects here, we instead employ an *ad hoc* softening in the Coulomb potential of the form $V(r) \propto (r^2 + \varepsilon^2)^{-1/2}$, where ε is some fraction of the interparticle spacing a_e. This allows us to verify analytical results in the classical ($\Gamma \ll 1$) regime, while at the same time giving a means of obtaining approximate scaling laws into the strongly coupled regime.

Due to the large mass ratio m_i/m_e between the electrons and ions the dynamics of the two species occur on rather different time scales. The time step has to be chosen according to the much quicker electron motion, ensuring that the paths of the particles are resolved accurately enough that collisions are correctly described. There are two limiting factors for this: the speed and the closeness of the particles. The time step has to be small enough to describe close encounters according to the softened force law. Taking $\Delta v \simeq 10\% \max(v_{te}, v_0)$ results in $\Delta t_f \leqslant \max(v_0, 1) f^2 N_D^{1/3}/Z$, where f is some fraction of the average interparticle spacing, typically 0.3–0.5. The other time step limitation is that the fastest particles should not move more than a distance $\Delta x = f a_e$, so that $\Delta t_s < f N_D^{-1/3}/[2\max(v_0, 1)]$. In the simulation the smaller of these two time steps is applied, so that $\Delta t = \min(\Delta t_s, \Delta t_f)$.

Periodic boundaries are handled in the usual way using an Ewald summation, which has previously been combined with both tree codes [43] and FMM codes [44]. However, for plasma applications the accuracy of the calculation has to be improved by including higher moments of the multipole expansion. A more detailed description of implementing the Ewald sum and higher moments of the force can be found in Refs. [45,40].

B. Constant temperature dynamics

The systems under consideration here are in a nonequilibrium state, because the applied electric field heats the system during the simulation. Although this heating is physical, it presents a problem because the state of the system changes disproportionately as the simulation evolves. Therefore, in order to sample or measure a variable in an *isothermal* system, one must either rescale the velocity distribution after a certain number of time steps, or modify the usual equation of

motion to compensate for the heating. Both methods physically correspond to immersing the whole system in an infinite heat bath. With velocity rescaling, assuming that the perturbation is oscillatory, this can be at every full cycle. Alternatively the rescaling can be performed at every time step—see Ref. [46] for a review of these methods.

In the simulations that follow in Sec. IV, we include the external force explicitly in the equation of motion by adding a Lagrange multiplier, so that for each particle species α,

$$\frac{d\boldsymbol{r}_\alpha}{dt}=\boldsymbol{v}_\alpha, \tag{9}$$

$$\frac{d\boldsymbol{v}_\alpha}{dt}=\boldsymbol{a}_\alpha-\xi_\alpha\boldsymbol{v}_\alpha, \tag{10}$$

where $\boldsymbol{a}$ is the acceleration due to both internal and external forces and ξ_α is to be determined by the constraint condition. The thermal energy of each particle species α is given by

$$U_\alpha^{\mathrm{therm}}=\frac{1}{2}m_\alpha\sum_i(\boldsymbol{v}_i^2-\langle\mathbf{v}_i\rangle^2). \tag{11}$$

Initially, for a 3D Maxwellian distribution we have in normalized units $U_{\mathrm{therm}}(t=0)=3N_e/2$. The electron temperature is then just $T_e=2U_{\mathrm{therm}}/3N_e$. Setting $dU_{\mathrm{therm}}/dt=0$, we arrive at the condition

$$\xi_\alpha=\frac{\sum\boldsymbol{v}_i\cdot\boldsymbol{a}_i-\sum\boldsymbol{v}_i\cdot\sum\boldsymbol{a}_i/N}{\sum\boldsymbol{v}_i^2-\left(\sum\boldsymbol{v}_i\right)^2/N}. \tag{12}$$

To implement this scheme, we follow Ref. [46] and split the velocity advance into two halves. Dropping the subscript α, we first perform an unconstrained half step:

$$\boldsymbol{v}'=\boldsymbol{v}^{n-1/2}+\frac{1}{2}\boldsymbol{a}^n\Delta t. \tag{13}$$

Next, we determine the new thermal energy U' according to Eq. (11) and then compute the ratio

$$\chi(t)=\sqrt{\frac{U_0}{U'(t)}}, \tag{14}$$

where U_0 is the desired (initial) thermal energy. It is straightforward to show that $\chi^{-1}=1+\xi\Delta t/2$, so that the second half step reduces to [47]

$$\boldsymbol{v}^{n+1/2}=(2\chi-1)\boldsymbol{v}^{n-1/2}+\chi\boldsymbol{a}^n\Delta t. \tag{15}$$

Since we are only concerned with electron dynamics here, we can neglect the heating of the ions (by taking a high mass ratio) and just apply Eqs. (9)–(15) to the electrons only. The technique can, however, be generalized to multispecies plasmas.

To illustrate the constraint method in action, we compare three simulations of inverse-bremsstrahlung heating all starting from the same initial conditions: $v_0=2.0$, $\Gamma=0.5$, $N_e=N_i=1000$, $Z=1$. The initial electron and ion positions were initialized using a Monte Carlo routine to place the system in its minimum potential energy configuration. If this is not done, or if insufficient MC ''moves'' are taken, the system will initially heat up as it relaxes to this state. Indeed, this is exactly what we observe in Fig. 2(a); the temperature increases from $T_e=1.0$ to 1.1 in a time $\sim 1.5\omega_p^{-1}$. Subsequently, the thermal energy increases steadily due to inverse-bremsstrahlung heating at a rate given by

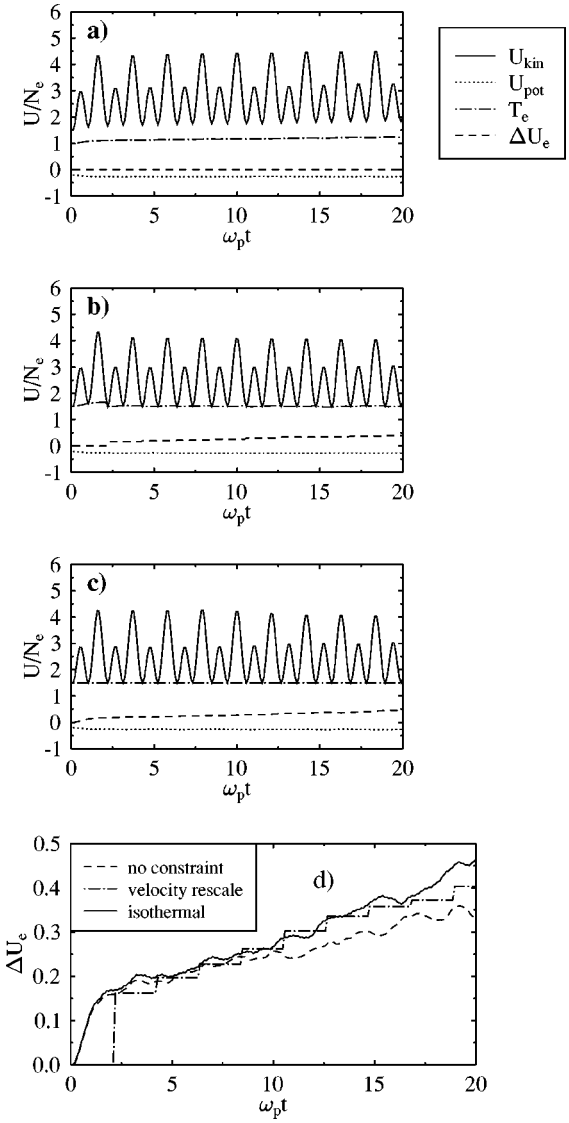

FIG. 2. Comparison of constraint schemes: (a) no constraint (energy conserving), (b) velocity rescaling, and (c) modified equation of motion with isothermal constraint. The simulation parameters were $\Gamma=0.5$, $v_0/v_{te}=2$, $\omega/\omega_p=3$, with 2000 particles. The heating curves are redrawn in (d) on an expanded scale for clarity.

$$\frac{\Delta U_e}{\Delta t}=\frac{\nu_{ei}v_0^2}{4}. \tag{16}$$

Thus, although we can still extract ν_{ei} in this case, we would actually have to rescale Γ by $(1.0/1.1)=0.9$ to describe the actual plasma conditions. This inconvenience can be mitigated to a certain extent by allowing the system to relax dynamically from a slightly higher Γ with the field switched off. A more serious problem is the temperature in-

crease which accompanies the IB heating. Because the collision frequency scales as $T_e^{-3/2}$, the heating rate decreases with time, and we are likely to underestimate ν_{ei} from the slope of the temperature curve in Fig. 2(d).

To get around this problem, two means of maintaining *isothermal* systems are implemented in our code. First and most simply, we can rescale the velocities at the end of each cycle such that

$$\boldsymbol{v}'_\alpha = \boldsymbol{v}_\alpha \sqrt{\frac{U_0}{U_{\rm therm}}}. \tag{17}$$

This is illustrated in Fig. 2(b), in which we see that after the initial relaxation, the temperature $T=2U/3$ now fluctuates around its nominal value $T_0=1.0$. The heating rate is now determined from the heat *removed* from the system due to velocity rescaling. Thus at the end of each cycle, we calculate

$$\Delta U_e = U_{\rm therm} - U_0, \tag{18}$$

which results in the somewhat jerky dashed curve in Fig. 2(b).

A smoother result can be obtained using the constant-temperature dynamics algorithm outlined earlier—Fig. 2(c). Here, we apply the velocity correction according to Eqs. (14) and (15) at each time step. Again, the heating corresponds to the energy removed, and is given by

$$\Delta U_e = 2(U' - U_0) = 2U_0[\chi(t)^{-2} - 1]. \tag{19}$$

On average, χ is just less than unity and the temperature increment per time step is small, so a large number of particles are generally needed to smooth out statistical fluctuations in ΔU_e. Most of the results which follow were obtained using this method, i.e., constant temperature dynamics. Thus both v_0 *and* v_{te} were effectively held constant while the heating rate was computed from Eq. (19).

IV. RESULTS: INVERSE-BREMSSTRAHLUNG HEATING

We now use the tree code with the modified dynamics described above to calculate the heating rate due to an applied oscillating field. This field is uniform in space and applied in the x direction: $E(t)=E_0 \sin \omega t$. For these simulations between 20 000 and 40 000 electrons and ions (with $Z=1$) were randomly placed in a cubic box and allowed to relax to an equilibrium state with the field switched off.

First we check that we recover the well-known classical result of Dawson and Oberman [Eq. (3)] for the weakly coupled regime $\Gamma=0.1$. This is done in Fig. 3, which shows the normalized collision frequency as a function of the coupling parameter for $\omega/\omega_p=3$. As we increase Γ, we find a departure from the classical result for $\Gamma \gtrsim 0.2$, essentially due to the usual limitation on the latter theory that the Coulomb logarithm ''becomes negative.'' Also shown for comparison is the analytic result of Cauble and Rozmus [20] who used a Debye-Hückel expansion *including* electron degeneracy effects to obtain corrections near $\Gamma=1$. Since we do not include quantum effects in these simulations, the results for $\Gamma>1$ should be treated with some caution: however, the curve does indicate a strong scaling with coupling parameter

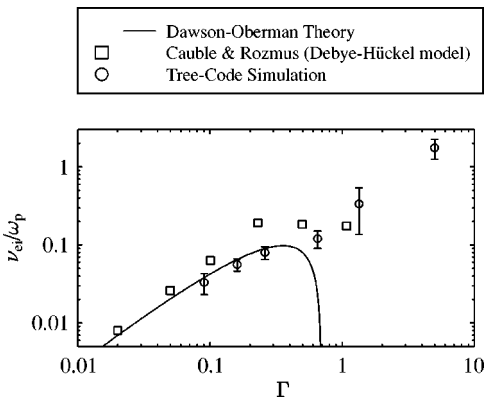

FIG. 3. Dependence of collision rate on coupling parameter for $Z=1$, $\omega/\omega_p=3$, and $v_0/v_{te}=0.2$. The simulation points are the circles with estimated error bars. Also shown are theoretical curves from Dawson and Oberman (Ref. [6]) and Cauble and Rozmus (Ref. [20]).

rather than a saturation predicted by most theories.

It should be stressed at this point that even though the primary motivation for using this code is the investigation of dense plasma effects, most of the results shown here are in fact calculated for the high-frequency ($\omega > \omega_p$) regime. To make a connection with the dc ($\omega \ll \omega_p$) conductivity relevant to short-pulse laser-solid interactions, we show the frequency dependence of ν_{ei} in Fig. 4. In the weak-coupling limit $\Gamma=0.1$, we see a clear resonance at ω_p as expected [48], below which the simulation points approach the classical dc limit [49]. For $\Gamma=0.65$ the behavior appears to be more complicated, with apparent enhancements of the collision rate for certain values of ω/ω_p. This behavior is presently not understood, and cannot be explained in terms of the correlation effects suggested by Decker *et al.* to account for their anomalous (PIC) results in a region where $x_0/\lambda_D > 1$ [12].

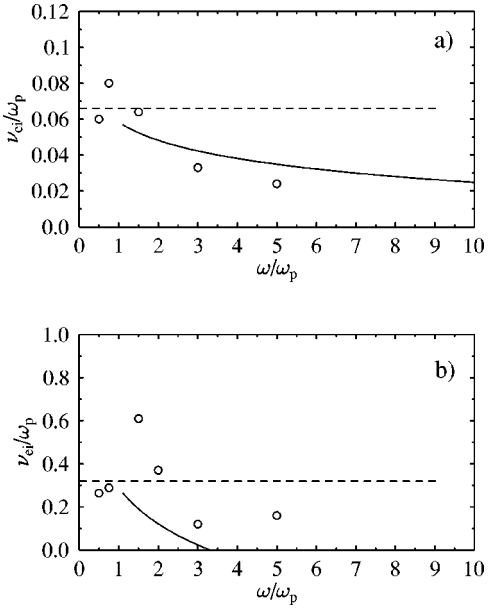

FIG. 4. Frequency dependence of collision rate for $v_0/v_{te}=0.2$: (a) weakly coupled system, (b) moderately coupled system. The solid and dashed curves represent the Dawson-Oberman theory and dc limit, respectively.

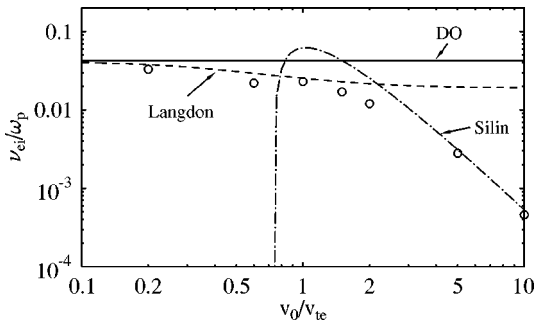

FIG. 5. Nonlinear inverse bremsstrahlung for $\Gamma=0.1$, $Z=1$: simulation results (circles) compared with classical theory after Dawson and Oberman (DO, Ref. [6]), DO theory with Langdon correction (Ref. [14]), and the high v_0/v_{te} limit due to Silin (Ref. [13]).

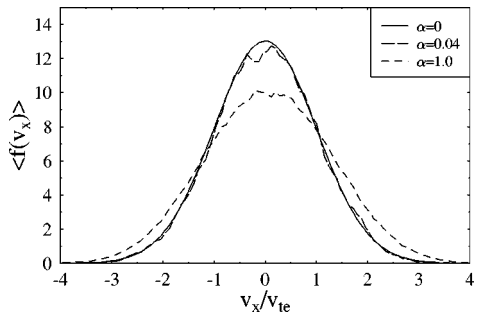

FIG. 6. Cycle-averaged distribution functions for weakly coupled plasma heated by inverse bremsstrahlung for $Z=1$ where $\alpha=Zv_0^2/v_{te}^2$.

We continue our study by extending the simulations into the nonlinear regime $v_0/v_{te}>1$ with $Z=1$. For the code, this involves no additional technical difficulty except that we must decrease the time step accordingly to accommodate the higher oscillation velocities of the electrons. Measuring the heating rate actually becomes easier because it is less prone to thermal fluctuations. The results for a weakly coupled system are shown in Fig. 5, and compared with the theoretical limiting cases of Dawson and Oberman (DO) [6] and Silin [13] for low and high v_0/v_{te}, respectively. Note that for $v_0/v_{te}\gtrsim 0.2$, the simulation points lie below the DO result, following instead the curve obtained by including Langdon's correction factor [14]. Although there is some numerical error associated with the simulation values, this is not more than 20% in this case. Some of the runs were also repeated with smaller time steps and potential-truncation parameters with no significant difference in the result. We conclude that the reduction in heating rate is indeed a consequence of the Langdon effect [14]—a distortion of the velocity distribution which occurs when the electron-electron collision rate is insufficient to bring the system back to a Maxwellian equilibrium.

To check this we computed the cycle-averaged distribution function for various v_0/v_{te}, the result of which is shown in Fig. 6. Departures from the initial Maxwellian distribution are already apparent for $v_0/v_{te}=0.2$, consistent with the predicted scaling with Zv_0^2/v_{te}^2 [14]. Strictly speaking, Langdon's theory is valid for simultaneously high Z and $v_0<v_{te}$, so we can only make a quantitative comparison for $v_0<v_{te}$ in Fig. 5. For $v_0/v_{te}\gg 1$, the simulation points approach the asymptotic curve predicted by Silin [13], confirming the assertion in Refs. [17] and [12] that the Langdon reduction is no longer effective in this regime.

It should be stressed that we make no assumptions about the distribution function except at the start of the calculation, where it is initialized as a Maxwellian. As the simulation proceeds, it is allowed to evolve self-consistently, including both *e-i and e-e* collisions, just as in a Fokker-Planck code. Some modification to the distribution function might occur due to the temperature constraint scheme, which, in its present implementation, does not discriminate between high and low velocities: the same ''correction'' factor is applied to all particles. On the other hand, we would only expect this to become significant for high Γ, where the heating rates are of the same order as the plasma frequency. To the best of our knowledge, the results in Figs. 5 and 6 represent the first *microscopic* verification of the Langdon effect.

V. CONCLUSIONS

To summarize, a simulation technique for modeling nonlinear transport processes in dense plasmas has been presented. The code reproduces standard theory in the weak-coupling limit and has the potential to check existing and future analytical models in the strong-coupling regime. In our investigation of inverse-bremsstrahlung absorption, we have not attempted to provide a definitive coverage of all parameter space (intensity, laser frequency, and coupling parameter) here; rather, we have indicated regions which would merit further investigation, for example, the high-intensity, strong-coupling regime now accessible with terawatt femtosecond lasers. To make accurate predictions of the plasma collisionality for specific temperatures and densities, however, one would need to include electron degeneracy effects in the model—a task which we reserve for future study. The plasma tree code can in principle also be used to calculate other transport coefficients, such as the thermal conductivity, dc electrical conductivity, as well as the equation of state in strongly coupled systems.

ACKNOWLEDGMENTS

This work was supported in part by the Deutsche Forschungsgemeinschaft and by the TMR program of the European Union, Contract No. ERBRMXCT960080. The simulations were performed on the Cray T90 at the HLRZ, Jülich. The authors also wish to thank A. R. Bell and M. G. Haines for useful discussions during the 1997 CECAM Workshop in Lyon, France.

APPENDIX: NORMALIZING UNITS

In order to avoid a Z dependence in the dimensionless variables, we have deliberately chosen normalizing factors based on the *electron* plasma parameters—principally the electron plasma frequency and Debye length. This system is appropriate for two-component plasma (TCP) modeling, where the physics is governed by electron motion, but it is still convenient to specify the system in terms of Γ and Z. A more natural length scale for a one-component plasma would

be $\lambda_{Di}=\{k_B T_e/4\pi n_i (Ze)^2\}^{1/2}$, in which case one obtains the identities $a_i/\lambda_{Di}=\sqrt{3\Gamma}$ and $N_{Di}=(3\Gamma)^{-3/2}$ for the mean ion separation and number of ions in a Debye sphere, respectively. To convert between our units and natural OCP units, we make use of the relations

$$a_i = Z^{1/3} a_e ,$$

$$\lambda_{Di} = Z^{-1/2} \lambda_D ,$$

$$N_{Di} = Z^{-5/2} N_D .$$

[1] M. D. Perry and G. Mourou, Science **264**, 917 (1994).
[2] M. D. Rosen, Phys. Fluids B **2**, 1461 (1990).
[3] R. Kodama, J. Appl. Phys. **59**, 3050 (1986).
[4] J. C. Kieffer, M. Chaker, J. P. Matte, H. Pépin, C. Y. C. Côté, Y. Beaudoin, T. W. Johnston, C. Y. Cien, S. Coe, G. Mourou, and O. Peyrusse, Phys. Fluids B **5**, 2676 (1993).
[5] J. Lindl, Phys. Plasmas **2**, 3933 (1995).
[6] J. Dawson and C. Oberman, Phys. Fluids **5**, 517 (1962).
[7] G. J. Pert, J. Phys. A **5**, 506 (1972).
[8] L. Schlessinger and J. Wright, Phys. Rev. A **20**, 1934 (1979).
[9] S. C. Rae and K. Burnett, Phys. Rev. A **46**, 2077 (1992).
[10] S. Pfalzner, Appl. Phys. B: Photophys. Laser Chem. **55**, 368 (1992).
[11] G. J. Pert, Phys. Rev. E **51**, 4778 (1995).
[12] C. D. Decker, W. B. Mori, and J. M. Dawson, Phys. Plasmas **1**, 4043 (1994).
[13] V. P. Silin, Zh. Eksp. Teor. Fiz. **47**, 2254 (1964) [Sov. Phys. JETP **20**, 1510 (1965)].
[14] A. B. Langdon, Phys. Rev. Lett. **44**, 575 (1980).
[15] J. R. Albritton, Phys. Rev. Lett. **50**, 2078 (1983); J. P. Matte, T. W. Johnston, J. Delettrez, and R. L. McCrory, *ibid.* **53**, 1461 (1984).
[16] J. M. Liu, J. S. De Groot, J. P. Matte, T. W. Johnston, and R. P. Drake, Phys. Rev. Lett. **72**, 2717 (1994).
[17] R. D. Jones and K. Lee, Phys. Fluids **25**, 2307 (1982).
[18] S. A. Uryupin, S. Kato, and K. Mima, Phys. Plasmas **2**, 3100 (1995).
[19] A. N. Mostovych, K. J. Kearney, J. A. Stamper, and A. J. Schmitt, Phys. Rev. Lett. **66**, 612 (1990).
[20] R. Cauble and W. Rozmus, Phys. Fluids **28**, 3387 (1985).
[21] S. Ichimaru and S. Tanaka, Phys. Rev. A **32**, 1790 (1985).
[22] D. B. Boercker, Phys. Rev. A **23**, 1969 (1981).
[23] M. Berkovsky, Y. K. Kurilenkov, and H. M. Milchberg, Phys. Lett. A **168**, 416 (1992).
[24] M. W. C. Perrot and F. Dharma-wardana, Phys. Rev. A **36**, 238 (1986).
[25] G. A. Rinker, Phys. Rev. A **37**, 1284 (1988).
[26] R. L. Shepherd, D. R. Kania, and L. A. Jones, Phys. Rev. Lett. **61**, 1278 (1988).
[27] S. G. Brush, H. L. Sahlin, and E. Teller, J. Chem. Phys. **45**, 2102 (1966).
[28] J. P. Hansen, I. R. McDonald, and P. Viellefosse, Phys. Rev. A **20**, 2590 (1979).
[29] W. L. Slattery, G. D. Doolen, and H. E. DeWitt, Phys. Rev. A **26**, 2255 (1982).
[30] J. M. Dawson, Rev. Mod. Phys. **55**, 403 (1983).
[31] C. Birdsall and A. Langdon, *Plasma Physics Via Computer Simulation* (McGraw-Hill, New York, 1985).
[32] A. R. Bell, R. Evans, and D. Nicholas, Phys. Rev. Lett. **46**, 243 (1981).
[33] J. P. Matte and J. Virmont, Phys. Rev. Lett. **49**, 1936 (1982).
[34] E. Epperlein, G. Rickard, and A. R. Bell, Comput. Phys. Commun. **52**, 7 (1988).
[35] J. P. Hansen and I. R. McDonald, Phys. Rev. A **23**, 2041 (1981).
[36] H. Furukawa and K. Nishihara, Phys. Rev. A **42**, 3532 (1990).
[37] J. Eastwood, R. W. Hockney, and D. N. Lawrence, Comput. Phys. Commun. **19**, 215 (1980).
[38] J. Barnes and P. Hut, Nature (London) **324**, 446 (1986).
[39] L. Hernquist, Comput. Phys. Commun. **48**, 107 (1988).
[40] S. Pfalzner and P. Gibbon, *Many Body Tree Methods in Physics* (Cambridge University Press, New York, 1996).
[41] J. Makino, J. Comput. Phys. **87**, 148 (1990).
[42] C. Deutsch, Phys. Lett. **60A**, 317 (1977).
[43] F. R. Bouchet and L. Hernquist, Astrophys. J. **400**, 25 (1992).
[44] K. E. Schmidt and M. A. Lee, J. Stat. Phys. **63**, 1223 (1991).
[45] S. Pfalzner and P. Gibbon, Comput. Phys. Commun. **79**, 24 (1994).
[46] M. P. Allen and D. J. Tildesley, *Computer Simulations of Liquids* (Oxford University Press, Oxford, 1987).
[47] D. Brown and J. H. R. Clarke, Mol. Phys. **51**, 1243 (1984).
[48] P. Kaw and A. Salat, Phys. Fluids **12**, 342 (1968).
[49] J. L. Spitzer, *Physics of Fully Ionized Gases* (John Wiley, New York, 1962).